

# Mint Proteins Are Required for Synaptic Activity-dependent Amyloid Precursor Protein (APP) Trafficking and Amyloid $\beta$ Generation\*

Received for publication, December 5, 2013, and in revised form, April 15, 2014. Published, JBC Papers in Press, April 17, 2014, DOI 10.1074/jbc.M113.541003

Sarah E. Sullivan, Gregory M. Dillon, Josefa M. Sullivan, and Angela Ho<sup>1</sup>

From the Department of Biology, Boston University, Boston, Massachusetts 02215

**Background:** Activity-dependent amyloid  $\beta$  ( $A\beta$ ) generation requires endosomal proteolytic cleavage of the amyloid precursor protein (APP).

**Results:** Mints are adaptor proteins that regulate APP endocytosis and insertion at the plasma membrane upon activity induction or inhibition.

**Conclusion:** Mints are necessary for activity-induced APP trafficking and  $A\beta$  generation.

**Significance:** Insight into the cell biology and molecules controlling APP trafficking is essential in understanding  $A\beta$  pathogenesis.

Aberrant amyloid  $\beta$  ( $A\beta$ ) production plays a causal role in Alzheimer disease pathogenesis. A major cellular pathway for  $A\beta$  generation is the activity-dependent endocytosis and proteolytic cleavage of the amyloid precursor protein (APP). However, the molecules controlling activity-dependent APP trafficking in neurons are less defined. Mints are adaptor proteins that directly interact with the endocytic sorting motif of APP and are functionally important in regulating APP endocytosis and  $A\beta$  production. We analyzed neuronal cultures from control and Mint knockout neurons that were treated with either glutamate or tetrodotoxin to stimulate an increase or decrease in neuronal activity, respectively. We found that neuronal activation by glutamate increased APP endocytosis, followed by elevated APP insertion into the cell surface, stabilizing APP at the plasma membrane. Conversely, suppression of neuronal activity by tetrodotoxin decreased APP endocytosis and insertion. Interestingly, we found that activity-dependent APP trafficking and  $A\beta$  generation were blocked in Mint knockout neurons. We showed that wild-type Mint1 can rescue APP internalization and insertion in Mint knockout neurons. In addition, we found that Mint overexpression increased excitatory synaptic activity and that APP was internalized predominantly to endosomes associated with APP processing. We demonstrated that presenilin 1 (PS1) endocytosis requires interaction with the PDZ domains of Mint1 and that this interaction facilitates activity-dependent colocalization of APP and PS1. These findings demonstrate that Mints are necessary for activity-induced APP and PS1 trafficking and provide insight into the cellular fate of APP in endocytic pathways essential for  $A\beta$  production.

Synaptic activity modulates the formation and secretion of  $A\beta$ <sup>2</sup> (1–3). Previous evidence indicates that enhanced neuronal activity increases  $A\beta$  production, whereas blocking neuronal activity decreases  $A\beta$  production (1). Neuronal activity-dependent  $A\beta$  production is largely mediated by clathrin-dependent endocytosis of surface APP, endosomal processing of APP, and  $A\beta$  release (3, 4). The sorting signal that regulates endocytic processing of APP required for  $A\beta$  generation is the highly conserved YENPTY consensus sequence for clathrin-coated pit internalization, located in the cytoplasmic region of APP (5). Knock-in mice lacking the YENPTY endocytic motif of APP or mice in which clathrin-mediated endocytosis is inhibited have reduced  $A\beta$  levels in the brain, indicating that endocytosis is critical for  $A\beta$  production (6, 7). Thus, understanding the cell biology and molecules controlling APP trafficking is of great significance for the mechanistic understanding of AD.

We propose that Mint proteins are critical players in regulating activity-dependent APP trafficking, which, in turn, affects  $A\beta$  generation. Mints 1–3, also referred to as X11 $\alpha/\beta/\gamma$ , X11/L1/L2, or APBA1/2/3, are multidomain adaptor proteins that interact with a variety of synaptic and Alzheimer-related proteins. In the variable N-terminal region, neuronal Mints 1 and 2 bind to Munc18-1, an essential synaptic fusion protein, linking Mints to synaptic vesicle exocytosis (8). In the conserved C terminus, all Mints contain a phosphotyrosine-binding domain that binds directly with the YENPTY endocytic motif of APP (9) and two PDZ domains that bind a number of proteins, including PS1, the catalytic core of  $\gamma$ -secretase that cleaves APP (10, 11). Several lines of evidence suggest that Mints play an important role in activity-dependent APP trafficking. 1) Mints bind directly to APP and regulate  $A\beta$  production because deletion of Mints decreases  $A\beta$  plaque production in the brains of aging mice and mouse models of AD (12); 2) APP endocytosis is

\* This work was supported, in whole or in part, by National Institute of Health Grants K01 AG027311 and R01 AG044499 (to A. H.). This work was also supported by Alzheimer's Association Grant IIRG-09-130591 (to A. H.).

<sup>1</sup> To whom correspondence should be addressed: Dept. of Biology, Boston University, 24 Cummings Mall, Boston MA. Tel.: 617-353-2093; Fax: 617-353-6340; E-mail: aho1@bu.edu.

<sup>2</sup> The abbreviations used are:  $A\beta$ , amyloid  $\beta$ ; APP, amyloid precursor protein; AD, Alzheimer disease; MTF, Mint triple-floxed; MTF<sup>tg</sup>, MTF carrying the double transgene of mutant APP and presenilin 1; DIV, days *in vitro*; PTX, picrotoxin; TTX, tetrodotoxin; mEPSC, miniature excitatory postsynaptic current.

attenuated in Mint knockout neurons, revealing a role for Mints in APP trafficking (13); 3) Mints are regulators of synaptic transmission because deletion of Mints decreases spontaneous miniature currents and neurotransmitter release at excitatory synapses (14, 15); 4) Mints are up-regulated and found in A $\beta$  plaques of post-mortem AD brains (16, 17); and 5) *MINT2* has been identified recently as a core regulatory mediator of APP endocytosis and metabolism associated with late-onset AD on the basis of whole-transcriptome cerebral cortex gene expression (18). Here we examined the cellular mechanism by which Mints regulate activity-induced APP trafficking that is relevant for A $\beta$  pathogenesis.

## EXPERIMENTAL PROCEDURES

**Plasmids**—For lentivirus production, individual full-length rat Mint 1–3 cDNAs were inserted into pEGFP-C3 (Clontech) and subsequently inserted into the pFUW lentiviral vector to generate the pFUW-EGFP-Mint1, pFUW-EGFP-Mint2, and pFUW-EGFP-Mint3 plasmids. Generation of pFUW-Mint1 $\Delta$ PDZ1/2 has been described previously (31).

**Neuronal Cultures and Lentiviral Infection**—We established two mouse lines that are homozygous for the floxed mutant alleles of all three *Mint* genes (Mint triple-floxed (MTF)) and MTF carrying the double transgene of the mutant *APP<sup>swe</sup>/PS1 $\Delta$ E9* that overproduce human A $\beta$  (MTF<sup>tg</sup>). High-density MTF and MTF<sup>tg</sup> hippocampal neurons were prepared from newborn mice of either sex and infected with lentiviruses as described previously (12–14). Briefly, neuronal cultures were infected with lentivirus at 3 days *in vitro* (DIV) and sustained until 13–15 DIV for analyses. The Mint1 rescue was performed by superinfection of *cre*-infected cultures with Mint1-expressing lentiviruses. All rescue experiments were performed with 3% lentivirus-expressing, GFP-tagged Mint1 protein. Wild-type neurons overexpressing individual Mints 1–3 were infected with 20% lentivirus-expressing, GFP-tagged Mint1, 2, or 3 proteins.

**Live Cell Internalization and Immunocytochemistry in Primary Neurons**—Neurons at 13–15 DIV were treated with either a 5-min pulse of 25  $\mu$ M glutamate, 150  $\mu$ M picrotoxin (PTX), or 2  $\mu$ M tetrodotoxin (TTX) for 1 h at 37 °C prior to antibody labeling. Live neurons were labeled with an antibody against the N-terminal epitope of APP (clone 22C11, Millipore), PS1 (MAB5232, Millipore), or GluR1 (Millipore) at 14 DIV. Briefly, neurons were washed with cold artificial cerebral spinal fluid (150 mM NaCl, 10 mM HEPES, 30 mM KCl, 2.6 mM CaCl<sub>2</sub>, 1 mM MgCl<sub>2</sub>, and 10 mM D-glucose (pH 7.4)) and incubated at 37 °C for 15 min to induce internalization as described previously (13). The remaining surface-bound antibodies were stripped in acid-stripping buffer (0.5 M NaCl and 0.2 M acetic acid) and fixed with 4% paraformaldehyde. Neurons were permeabilized in 0.3% Triton-X-100 and incubated with goat anti-mouse secondary antibodies conjugated to Alexa Fluor 546 (Invitrogen). For colocalization studies, following the PS1 internalization assay, neurons were incubated with primary anti-APP antibodies (U955) overnight at 4 °C prior to incubation with an Alexa Fluor 633-conjugated secondary antibody. For surface-expressed APP, neurons were fixed, and the surface-expressed APP was labeled with anti-APP antibodies (clone 22C11, Milli-

pore) and an Alexa Fluor 546-conjugated secondary antibody. All immunofluorescence images were captured by a FluoView FV10i scanning confocal microscope using a 60 $\times$  objective with 3 $\times$  optimal zoom, with laser gain and threshold filters kept constant between conditions. Z-stacks were acquired from top to bottom of neurons using a 0.25- $\mu$ m step with a numerical aperture of 1.5. Image analysis was performed using ImageJ software (National Institutes of Health). Internalization was measured by manual selection of the most central image from the Z-stack, and pixel intensity was quantified. The total soma areas were outlined manually from a non-experimental channel and overlaid onto the experimental channel prior to measuring intensity. The mean pixel intensity was divided by the soma area to eliminate variability because of varying soma sizes. Surface and insertion quantifications were taken from compressing the Z-stack into a single image and measuring the pixel intensity of the total captured soma area. For colocalization of internalized PS1 and APP, images were acquired as above, with cross-talk correction activated to prevent signal bleed. Images were acquired at 512  $\times$  512 pixels, with a single pixel representing 0.137  $\mu$ m. The JaCoP plugin for ImageJ was applied to unprocessed, center-selected images from acquired Z-stacks, and the degree of signal overlap was determined by Mander's coefficient.

**Insertion Assay**—The insertion assay was performed at 14 DIV as described previously (13). Briefly, live neurons were first incubated with the N-terminal epitope of APP (22C11, Millipore) for 15 min, followed by a cold (non-conjugated) secondary antibody for an additional 15 min to block preexisting cell surface APP. Neurons were then incubated for 15 min at 37 °C, fixed with 4% paraformaldehyde, and stained with the same APP antibody and an Alexa Fluor 546 secondary antibody. Newly inserted APP was visualized by a scanning confocal microscope with constant laser and threshold settings, and pixel intensity was quantified using ImageJ software.

**Electrophysiological Analysis**—Whole-cell voltage clamp analysis was performed in cultured hippocampal neurons at 13–16 DIV as described previously (14, 19). Briefly, synaptic recordings were filtered in electrode solution containing 105 mM Cs-MeSO<sub>3</sub>, 10 CsCl, 5 NaCl, 10 HEPES, 0.2 EGTA, 4 Mg-ATP, and 0.3 Na<sub>2</sub>GTP (pH 7.4) at 300 mosmol. Spontaneous event recordings were recorded in the presence of 1  $\mu$ M TTX and 50  $\mu$ M D-2-amino-5-phosphonovaleric acid plus 20  $\mu$ M bicuculline for miniature excitatory postsynaptic currents (mEPSCs). Glutamate-evoked recordings were recorded in the presence of 50  $\mu$ M cyclothiazide to additionally block AMPA receptor desensitization. Glutamate at 100  $\mu$ M was perfused into the bath until the evoked current stabilized. The total glutamate-evoked current was calculated as the difference between the peak and leak-evoked current, which was determined from the current before and after glutamate application. Recordings were acquired with an Axopatch 200A amplifier and Clampex 10.0 software (Molecular Devices).

**A $\beta$  Peptide Measurement**—MTF<sup>tg</sup> neurons at 13–15 DIV were treated with either 150  $\mu$ M PTX or 2  $\mu$ M TTX for 1 h. Conditioned medium was collected and centrifuged at 15,000  $\times$  g for 10 min at 4 °C. The supernatant was subjected to ELISA measurement for

## Activity-dependent APP Trafficking by Mints

human A $\beta$ 42 according to the instructions of the manufacturer (catalog no. 27711, ImmunoBiological Laboratories).

**Antibodies**—The following antibodies were used: APP 22C11 (catalog no. MAB348, Millipore), APP U955, GluR1-NT (catalog no. MAB2263, Millipore), Mint1 P730, Mint2 (catalog no. M3319, Sigma), Mint3 (catalog no. PA1-072, Thermo Scientific), PS1 (catalog no. MAB5232, Millipore), and tubulin DM1A (catalog no. T6199, Sigma). APP U955 and Mint1 P730 were gifts from Dr. T. C. Südhof.

**Statistical Analysis**—We used Tukey's test to determine statistical significance (\*,  $p < 0.05$ ; \*\*,  $p < 0.01$ ; \*\*\*,  $p < 0.001$ ).

## RESULTS

**Mints Are Required for Activity-induced APP Trafficking**—We first examined whether Mints play a role in activity-dependent APP endocytosis. A live cell endocytosis assay was performed to quantify intracellular APP in cultured neurons from established mouse lines that are homozygous for the floxed mutant alleles of all three Mint genes (MTF) and MTF carrying the double transgene of mutant APP and PS1 (*APP<sup>swe</sup>/PS1 $\Delta$ E9*) that overproduce human A $\beta$  (MTF<sup>tg</sup>). We have shown previously that cultured neurons from newborn mice infected with lentiviruses that expressed a functional *cre* recombinase showed complete deletion of all Mints, whereas neurons infected with inactive *cre* recombinase retain endogenous Mint expression (Fig. 6B and Refs. 12–14). Following glutamate application at 13–15 DIV, control MTF neurons showed an ~17 and 33% increase in internalized APP in the somas and processes, respectively, demonstrating that enhanced synaptic activity increases endogenous APP endocytosis (Fig. 1, A–C).

We next examined whether activity-induced APP endocytosis requires Mints. Under basal conditions, Mint knockout neurons showed a 23–28% reduction in internalized APP compared with control neurons, demonstrating that Mints regulate APP internalization, which supports our previous studies (13). Interestingly, Mint knockout neurons showed no additional changes in APP internalization following glutamate application. As a control, no visible staining was observed in non-permeabilized cells or cells treated with the endocytic inhibitor dynasore (data not shown).

In supporting experiments, addition of PTX, a noncompetitive GABA<sub>A</sub> receptor antagonist, to increase synaptic transmission caused a 31–34% increase in internalized APP in control MTF neurons (Fig. 1, D–F). In contrast, Mint knockout neurons prevented the increase in APP internalization following PTX application, suggesting that Mints play an important role in activity-induced APP internalization.

Because studies have shown differences in APP sorting pathways as a result of mutations that overproduce A $\beta$  levels (20, 21), we examined APP endocytosis using MTF<sup>tg</sup> neurons carrying the *APP<sup>swe</sup>/PS1 $\Delta$ E9* transgene. Consistent with our findings, we found an increase in internalized APP in MTF<sup>tg</sup> neurons following glutamate treatment (Fig. 1, G–I). Mint knockout neurons showed a significant reduction in internalized APP compared with MTF<sup>tg</sup> control neurons and were not affected upon glutamate application.

To determine whether Mints regulate activity-induced APP surface levels, both MTF and MTF<sup>tg</sup> neurons were fixed follow-

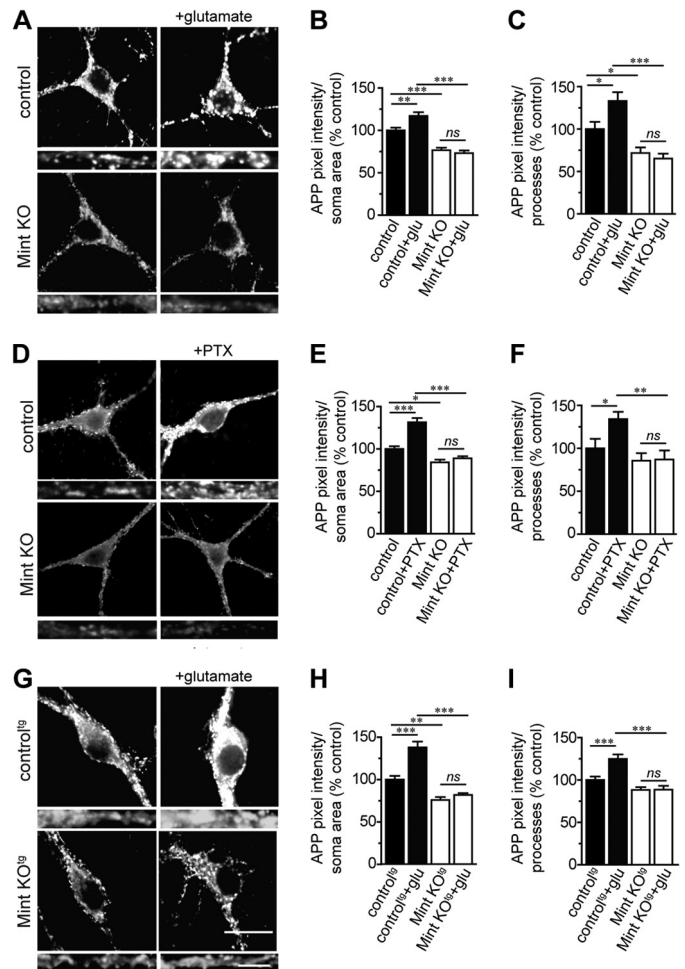


**FIGURE 1. Mint proteins regulate activity-dependent APP endocytosis.** MTF and MTF<sup>tg</sup> neurons were infected with lentiviral inactive (control) or active *cre* recombinase to delete all Mint proteins (*Mint KO*). Live cell endocytosis assay of neurons were labeled with an extracellular N-terminal APP antibody (22C11) and treated with 25  $\mu$ M glutamate (*glu*) for 5 min or 150  $\mu$ M PTX for 1 h at 37 °C to depolarize neurons. Proteins were internalized for 15 min at 37 °C before stripping of excess surface antibody and fixation. *A*, representative images of MTF control and Mint KO neurons following glutamate treatment. *Bottom panels*, representative images of processes. *B* and *C*, internalized APP immunostaining was visualized by confocal microscopy and quantified as a measure of pixel intensity within defined somas or processes and expressed as percent control ( $n = 2/132$  represents the number of independent experiments/total number of neurons assessed). *D*, representative images of MTF control and Mint KO neurons following PTX treatment. *E* and *F*, quantification of APP pixel intensity within defined somas or processes ( $n = 3/373$ ). *G*, representative images of MTF<sup>tg</sup> control and Mint KO neurons following glutamate treatment. *H* and *I*, quantification of APP pixel intensity within defined somas or processes ( $n = 4/218$ ). Scale bars = 20  $\mu$ m (somas) and 5  $\mu$ m (processes). \*,  $p < 0.05$ ; \*\*,  $p < 0.01$ ; \*\*\*,  $p < 0.001$ ; ns, not significant.

ing a 5-min treatment with glutamate, and the surface-exposed APP was immunolabeled with anti-APP antibodies. Surface APP staining showed no difference between control and Mint knockout neurons, and glutamate stimulation failed to alter APP surface staining in both MTF and MTF<sup>tg</sup> neurons (Fig. 2, A–D). The finding that activity controls APP endocytosis without significantly affecting steady-state surface expression suggests that membrane insertion of APP might also be regulated by activity. Newly inserted APP could arise from stable intracellular pools or by recycling of recently internalized APP. To examine whether neuronal activity affects APP inser-

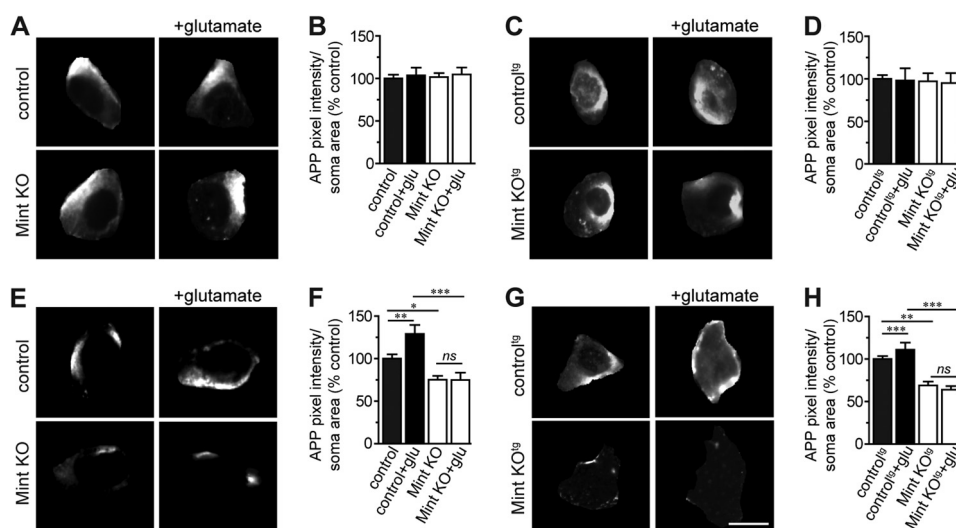


**FIGURE 2. Mints regulate activity-induced APP insertion at the plasma membrane.** *A–D*, surface APP immunostaining following glutamate stimulation in control and Mint KO neurons. *glu*, glutamate. *A* and *B*, MTF control and Mint KO neurons and quantification of APP pixel intensity within defined somas ( $n = 2/65$  represents the number of independent experiments/total number of neurons assessed). *C* and *D*, MTF<sup>19</sup> control and Mint KO neurons and quantification of APP pixel intensity within defined somas ( $n = 3/74$ ). *E–H*, live cell recycling assay following glutamate treatment in MTF and MTF<sup>19</sup> neurons. After blocking existing cell surface APP with primary antibody (22C11) and cold (non-fluorescence-conjugated) secondary antibody, neurons were incubated at 37 °C for 15 min. Following fixation, newly inserted APPs were labeled with the same APP antibody, visualized using fluorescent-conjugated secondary antibody, and then APP pixel intensity was quantified within defined somas. *E* and *F*, MTF control and Mint KO neurons and quantification of APP pixel intensity within defined somas ( $n = 2/136$ ). *G* and *H*, MTF<sup>19</sup> control and Mint KO neurons and quantification of APP pixel intensity within defined somas ( $n = 2/120$ ). Scale bars = 20  $\mu$ m (somas) and 5  $\mu$ m (processes). \*,  $p < 0.05$ ; \*\*,  $p < 0.01$ ; \*\*\*,  $p < 0.001$ ; ns, not significant.

tion into the plasma membrane and to measure the effect of synaptic activity on insertion, we performed insertion assays. We found newly inserted APP staining on the surface of somas that represent a rapid, constitutive insertion of APP into the plasma membrane in control neurons. Following glutamate application, control neurons showed an increase in APP insertion, demonstrating that enhancing synaptic activity accelerated the amount of newly inserted APP in the plasma membrane (Fig. 2, *E–H*). Under basal conditions, Mint knockout neurons showed a significant reduction in APP insertion compared with control neurons, demonstrating that Mints are necessary for the facilitation of APP insertion. Mint knockout neurons did not show any additional changes in APP insertion following glutamate application, suggesting that Mints are essential for glutamate-induced APP insertion into the plasma membrane.

**Mints Are Required for TTX-induced APP Trafficking**—To examine whether decreasing synaptic activity alters APP internalization, cultured MTF and MTF<sup>19</sup> neurons were treated with TTX, a sodium channel blocker that inhibits action potentials. TTX dramatically reduced APP internalization in the somas and processes of control MTF and MTF<sup>19</sup> neurons, demonstrating that inhibiting activity can decrease APP endocytosis (Fig. 3). As expected, Mint knockout neurons showed a reduction in internalized APP compared with control neurons under basal conditions. In addition, TTX treatment failed to alter APP internalization in Mint knockout neurons. Also, TTX had no effect on the steady-state amount of APP at the cell surface in both control and Mint knockout neurons (Fig. 4, *A–D*). However, the insertion of APP was decreased significantly in the presence of TTX in control MTF and MTF<sup>19</sup> neurons (Fig. 4, *E–H*). In addition, we found that TTX treatment does not affect APP insertion in Mint knockout neurons. Together, these

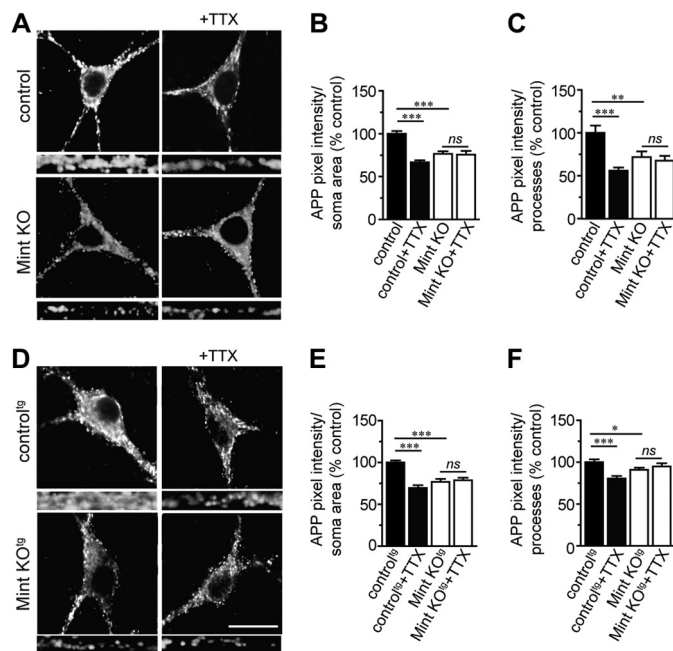


**FIGURE 3. TTX failed to alter APP endocytosis in Mint knockout neurons.** Neurons were treated with 2  $\mu$ M TTX for 1 h to reduce synaptic activity prior to live cell immunostaining. *A*, representative images of MTF control and Mint KO neurons. *Bottom panels*, representative images of processes. *B* and *C*, internalized APP immunostaining was quantified as a measure of pixel intensity within defined somas or processes, respectively, and expressed as percent control ( $n = 2/118$  represents the number of independent experiments/total number of neurons assessed). *D*, MTF<sup>19</sup> control and Mint KO neurons. *E* and *F*, quantification of APP pixel intensity within defined somas or processes, respectively ( $n = 4/295$ ). Scale bars = 20  $\mu$ m (somas) and 5  $\mu$ m (processes). \*,  $p < 0.05$ ; \*\*,  $p < 0.01$ ; \*\*\*,  $p < 0.001$ ; ns, not significant.

experiments suggest that APP trafficking can be controlled by synaptic activity and that Mints are essential for activity-induced APP trafficking.

## Activity-dependent APP Trafficking by Mints

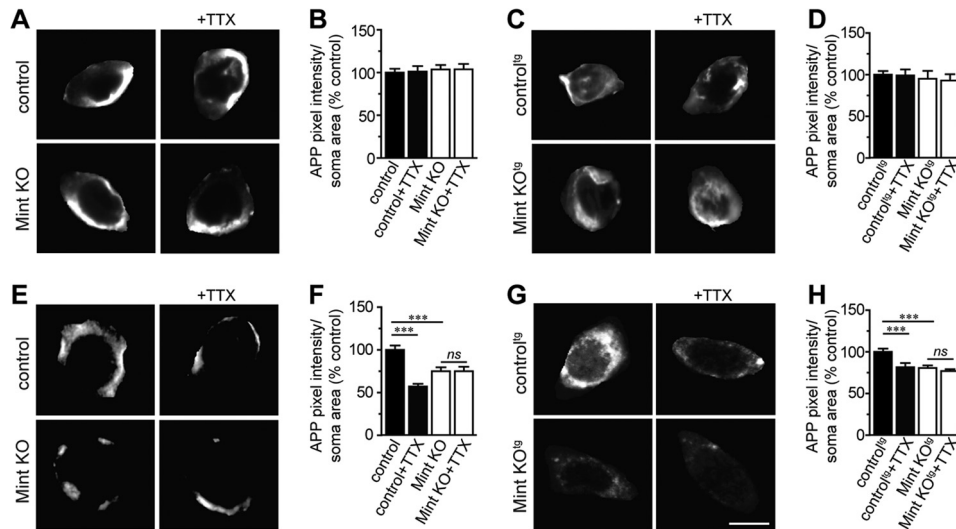


**FIGURE 4. APP insertion is decreased in TTX-treated neurons.** *A–D*, surface APP immunostaining. *A* and *B*, MTF control and Mint KO neurons and quantification of APP pixel intensity within defined somas ( $n = 2/160$  represents the number of independent experiments/total number of neurons assessed). *C* and *D*, MTF<sup>tg</sup> control and Mint KO neurons and quantification of APP pixel intensity within defined somas ( $n = 2/86$ ). *E* and *F*, MTF control and Mint KO neurons and quantification of APP pixel intensity within defined somas ( $n = 2/52$ ). *G* and *H*, MTF<sup>tg</sup> control and Mint KO neurons and quantification of APP pixel intensity within defined somas ( $n = 3/95$ ). Scale bars = 20  $\mu\text{m}$  (somas) and 5  $\mu\text{m}$  (processes). \*,  $p < 0.05$ ; \*\*,  $p < 0.01$ ; \*\*\*,  $p < 0.001$ ; ns, not significant.

*Mints Specifically Affect APP Trafficking*—To determine whether Mints have a specific effect on APP trafficking or cause a more general effect on endocytosis, we examined the internalization of the excitatory glutamate AMPA-type receptor GluR1, a protein that is internalized independently of Mints. Under basal conditions, GluR1 undergoes endocytosis, and we found no changes in GluR1 internalization in Mint knockout neurons (Fig. 5, *A–C*). Increasing synaptic activity with glutamate accelerated GluR1 internalization to 170 and 180% in the somas and processes of control MTF<sup>tg</sup> neurons, respectively. Conversely, blocking synaptic activity with TTX significantly reduced GluR1 internalization in control neurons. Under each pharmacological condition, GluR1 displayed similar endocytosis in Mint knockout neurons compared with the control, indicating that Mints do not affect GluR1 trafficking or endocytosis in general.

To exclude the possibility that Mint proteins could affect glutamate receptor function, we measured whole-cell currents to exogenous glutamate application in control and Mint knockout MTF<sup>tg</sup> neurons (Fig. 5, *D–E*). Glutamate application induced an inward current at a holding potential of  $-70$  mV. To eliminate differences in cell size, currents were normalized by cell capacitance and expressed as current densities. No difference in current density was detected after glutamate application in control and Mint knockout neurons.

*Mints Are Essential and Directly Involved in Activity-dependent APP Trafficking and  $A\beta$  Generation*—To determine whether Mints are essential and directly involved in activity-dependent  $A\beta$  generation, we examined 13–15 DIV control and Mint knockout MTF<sup>tg</sup> neurons following PTX or TTX treatment, pharmacological agents to increase or decrease neuronal activity, respectively. We found that  $A\beta_{42}$  levels were decreased significantly in the conditioned medium of Mint knockout neurons, supporting our previous findings (Fig. 6*A* and Ref. 12). Addition of PTX increased  $A\beta$  generation in con-

trol neurons, as reported previously (1). Interestingly, PTX failed to increase  $A\beta$  generation from Mint knockout neurons. Furthermore, decreasing neuronal activity by TTX significantly decreased secreted  $A\beta$  levels in control but not in Mint knockout neurons. We next examined whether synaptic activity affects the overall protein expression of Mints and APP. Both TTX and glutamate had no effect on total protein expression of Mints 1–3 and APP (Fig. 6*B*). In addition, we did not detect any changes in APP protein expression in Mint knockout neurons.

To directly probe whether Mints are essential and directly involved in activity-dependent APP trafficking, we performed rescue experiments with full-length Mint1 in cultured MTF<sup>tg</sup> neurons. Rescue experiments were performed by transfecting neurons with lentiviruses expressing GFP-tagged Mint1, proteins and active or inactive *cre* recombinase. Immunoblotting of Mint1 demonstrated that culture medium containing 3% lentivirus-expressing GFP-tagged Mint1, in Mint knockout neurons, showed a similar protein expression level as endogenous control neurons (Fig. 6*C*). Therefore, all rescue experiments were performed with 3% lentivirus-expressing GFP-tagged Mint1 protein. We found that increasing the amount of lentivirus GFP-tagged Mint1 protein did not affect the overall protein expression of APP. Electrophysiologically, we found that deletion of Mint proteins caused an  $\sim 2$ -fold decrease in the frequency, but not amplitude, of spontaneous mEPSCs, as described previously (Fig. 6, *D–F*) (14). Importantly, this decrease in excitatory synaptic transmission could be rescued to control levels with full-length Mint1.

We next tested rescue of the Mint knockout phenotype on APP endocytosis and insertion following glutamate and TTX application. Expression of wild-type Mint1 fully reversed the impairment in APP internalization and insertion in Mint knockout neurons demonstrating that Mints directly function in activity-dependent APP trafficking (Fig. 7).

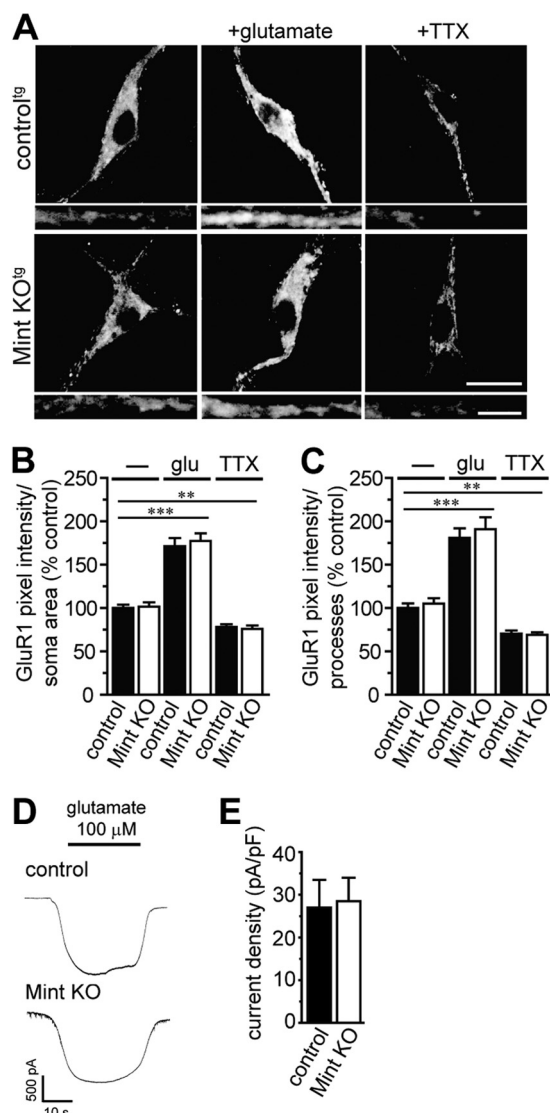


**FIGURE 5. Mints do not affect glutamate receptor trafficking and function.** Shown is a live cell endocytosis assay of MTF<sup>19</sup> neurons incubated with an extracellular N-terminal GluR1 antibody and subsequently treated with 25  $\mu$ M glutamate (*glu*) for 5 min at 37 °C or with 2  $\mu$ M TTX for 1 h prior to live cell immunostaining. *A*, representative images of MTF<sup>19</sup> control and Mint KO neurons treated with glutamate and TTX. *Bottom panels*, representative images of processes. *B* and *C*, internalized GluR1 immunostaining was quantified as a measure of pixel intensity within defined somas or processes and expressed as percent control ( $n = 3/307$  represents the number of independent experiments/total number of neurons assessed). *D*, whole-cell currents to exogenous glutamate application in MTF<sup>19</sup> control and Mint KO neurons at a holding potential of  $-70$  mV. *E*, no difference in current density was detected in glutamate-induced currents in control and Mint KO neurons. pA, picoamperes; pF, picofarad. Scale bars = 20  $\mu$ m (somas) and 5  $\mu$ m (processes). \*\*,  $p < 0.01$ ; \*\*\*,  $p < 0.001$ .

**Overexpression of Mints Enhanced Excitatory Synaptic Transmission and Accelerated APP Endocytosis and Insertion**—To determine whether overexpression of Mints alters neurotransmitter release, we infected wild-type neurons with lentivirus for Mints 1, 2, or 3 (Fig. 8*A*) and monitored synaptic transmission. Neurons overexpressing Mints 1–3 showed a significant increase in the frequency and amplitude of spontaneous mEPSCs (Fig. 8, *B* and *C*). These results suggest that the enhanced effects of Mint overexpression are due to an increase in the number of functional synapses at either presynaptic and/or postsynaptic sites.

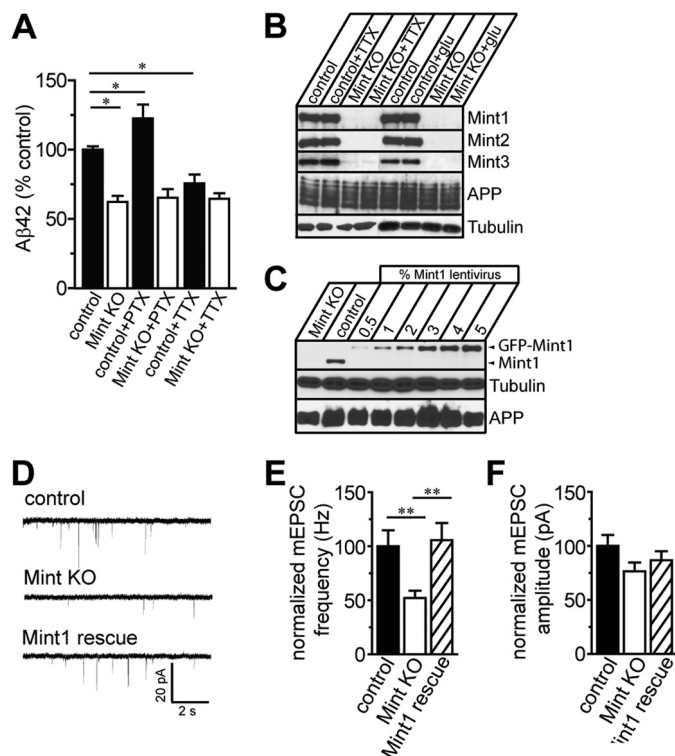


**FIGURE 6. Mints are necessary for activity-dependent A $\beta$  generation.** *A*, A $\beta$ 42 ELISA measurement from conditioned medium of MTF<sup>19</sup> control and Mint KO neurons following 1 h of PTX and TTX treatment at 37 °C. *B*, representative immunoblot analyses of lysates from MTF<sup>19</sup> control and Mint KO neurons treated with TTX or glutamate (*glu*). Lysates probed for individual Mint proteins show efficient deletion of Mints 1–3 in Mint KO neurons. *C*, expression of Mint1 in MTF<sup>19</sup> Mint KO neurons examined by immunoblotting of neurons treated with increasing percentages of GFP-Mint1 lentivirus. *D–F*, sample traces of mEPSC in MTF control, Mint KO, and Mint1 rescue neurons. The bar graphs indicate mEPSC frequency and mEPSC amplitude, respectively ( $n = 3/55$  represents the number of independent experiments/total number of neurons assessed). \*,  $p < 0.05$ ; \*\*,  $p < 0.01$ .

To examine the effect of Mint overexpression on APP trafficking, we performed live-cell immunostaining. Overexpression of individual Mints significantly enhanced APP internalization in the somas and processes of neurons compared with control neurons (Fig. 8, *D*, *F*, and *G*). Interestingly, the increased APP endocytosis in Mint-overexpressed neurons was prevented by the addition of TTX, indicating that synaptic activity had a significant effect on the efficiency of APP internalization (Fig. 8, *E–G*). We detected no significant differences between control and Mint-overexpressing neurons in surface APP (Fig. 9, *A* and *C*) but observed a large increase in APP insertion in Mint-overexpressing neurons (Fig. 9, *B* and *D*), suggesting that a significant fraction of APP is inserted into the plasma membrane and that the extent of APP endocytosis and insertion is increased by Mint overexpression.

**Mints Are Required for PS1 Internalization and Activity-dependent APP/PS1 Colocalization**—Because the PDZ domains of Mint1 have been shown to interact with PS1 (10, 11), we hypothesized that Mints also regulate PS1 trafficking. Therefore, we performed a live-cell endocytosis assay to quantify the relative amount of endocytosed PS1. MTF<sup>19</sup> control and Mint knockout neurons were incubated with an antibody against the extracellular loop domain of PS1. Under basal conditions, Mint knockout neurons showed a 27% decrease in internalized PS1,

## Activity-dependent APP Trafficking by Mints

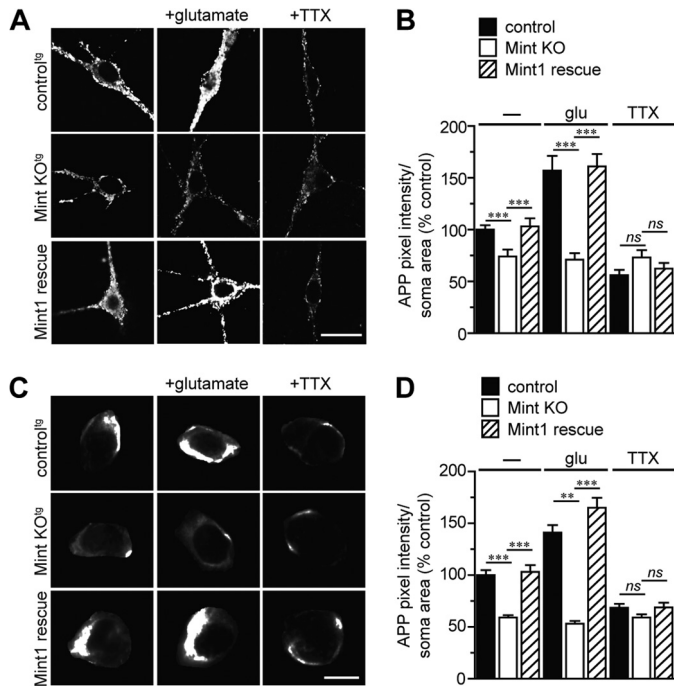


**FIGURE 7. Mints are directly involved in activity-dependent APP trafficking.** *A* and *B*, live cell endocytosis assay. MTF<sup>tg</sup> control, Mint KO, and Mint1 rescue neurons were treated with glutamate (*glu*) or TTX. Internalized APP immunostaining was quantified as a measure of pixel intensity within defined somas and expressed as percent control ( $n = 4/664$ ). *C* and *D*, live cell recycling assay. Shown are representative images and quantification of APP pixel intensity within defined somas ( $n = 2/337$ ). Scale bars = 20  $\mu\text{m}$ . \*\*,  $p < 0.01$ ; \*\*\*,  $p < 0.001$ ; *ns*, not significant.

suggesting that Mints regulate PS1 internalization (Fig. 10, *A* and *B*). To determine whether Mints are essential and directly involved in PS1 internalization, we performed rescue experiments with full-length Mint1 by coinfecting neurons with lentiviruses expressing GFP-tagged Mint1 proteins and active *cre* recombinase. Expression of wild-type Mint1 fully reversed the impairment in PS1 internalization in Mint knockout neurons (Fig. 10, *A* and *B*). We then tested whether PS1 binding to the Mint1 PDZ domains is required for Mint-dependent PS1 internalization by expressing a mutant Mint1 protein in which the PDZ1 and 2 domains have been truncated (Mint1 $\Delta$ PDZ1/2). Mint1 $\Delta$ PDZ1/2 impaired rescue, indicating that Mint1 interaction with PS1 is necessary to regulate PS1 trafficking.

Next, we examined whether synaptic activity regulates PS1 internalization. Following glutamate application, control neurons showed an  $\sim 25\%$  increase in internalized PS1, demonstrating that enhanced synaptic activity increases endogenous PS1 endocytosis (Fig. 10, *C* and *D*). Interestingly, we found that glutamate application failed to increase PS1 internalization in Mint knockout neurons.

To determine whether enhanced synaptic activity induce APP/PS1 colocalization, we immunolabeled with APP antibody after live-cell PS1 endocytosis assay upon glutamate stimulation. Quantitative analysis of confocal images revealed a 78% increase of internalized PS1 staining overlapping with APP in control neurons following glutamate induction (Fig. 10*C*, *E*). Mint knock-out neurons showed no changes in APP/PS1 colocalization with glutamate stimulation suggesting that Mints

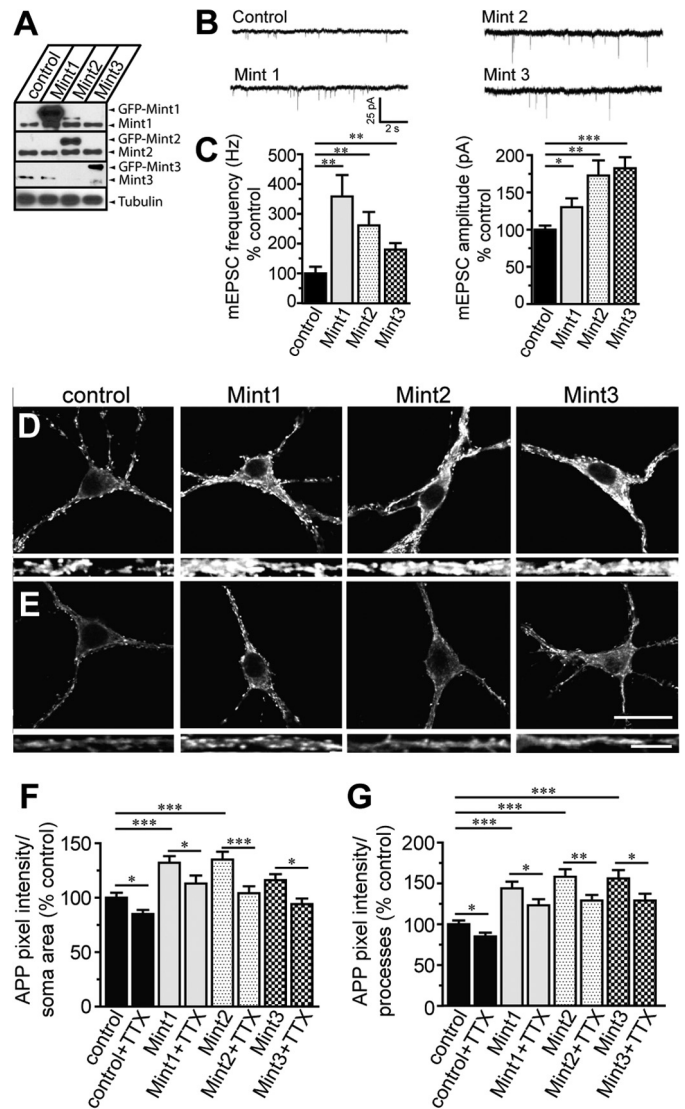


**FIGURE 8. Mint overexpression increases excitatory synaptic transmission and regulates APP endocytosis.** *A*, representative immunoblot analyses of lysates from wild-type neurons infected with lentiviral GFP-Mint 1, 2, or 3. Lysates probed for individual Mint proteins show expression of endogenous and overexpressed Mint proteins. *B*, sample traces showing mEPSCs of neurons infected with individual Mint proteins in wild-type neurons. *C*, bar graphs of mEPSC frequency and amplitude, respectively ( $n = 3/77$  represents the number of independent experiments/total number of neurons assessed). *D*, live cell endocytosis assay. Representative images of wild-type control and Mint1-, 2-, and 3-overexpressing neurons. *Bottom panels*, representative images of processes. *E*, wild-type control and Mint1-, 2-, and 3-overexpressing neurons treated with TTX for 1 h prior to live cell immunostaining. *Bottom panel*, representative images of processes. *F* and *G*, internalized APP immunostaining was quantified as a measure of pixel intensity within defined somas or processes and expressed as percent control ( $n = 2/343$ ). Scale bars = 20  $\mu\text{m}$  (somas) and 5  $\mu\text{m}$  (processes). \*,  $p < 0.05$ ; \*\*,  $p < 0.01$ ; \*\*\*,  $p < 0.001$ .

may play an important role in activity-induced APP/PS1 colocalization favoring A $\beta$  generation.

## DISCUSSION

This study identifies Mint proteins as an essential mechanistic component of activity-dependent APP trafficking and A $\beta$  generation. Neuronal stimulation by glutamate or PTX increases APP endocytosis and insertion, thus stabilizing APP at the plasma membrane (Figs. 1 and 2). Conversely, suppres-

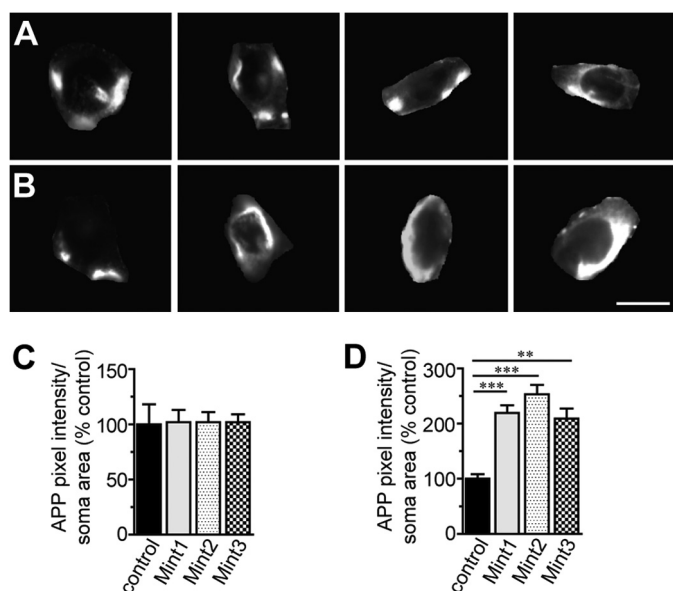


**FIGURE 9. Mint-overexpressing neurons increases APP insertion.** A and C, surface APP immunostaining. Shown are wild-type control and Mint1-, 2-, and 3-overexpressing neurons and quantification of APP pixel intensity within defined somas ( $n = 3/87$  represents the number of independent experiments/total number of neurons assessed). B and D, live cell recycling assay. Shown are wild type control and Mint1-, 2-, and 3-overexpressing neurons and quantification of APP pixel intensity within defined somas ( $n = 2/102$ ). Scale bars = 20  $\mu\text{m}$  (somas) and 5  $\mu\text{m}$  (processes). \*\*,  $p < 0.01$ ; \*\*\*,  $p < 0.001$ .

sion of neuronal activity by TTX decreases APP endocytosis and insertion (Figs. 3 and 4). Importantly, we demonstrate that Mints are required for activity-dependent APP trafficking, given that activity-dependent APP endocytosis and insertion were blocked in Mint knockout neurons. The effect of Mint deletion on APP internalization was not due to an overall effect on endocytosis because AMPA-type GluR1 internalization was unaffected in Mint knockout neurons (Fig. 5). In addition, we show that Mints are required for activity-dependent  $A\beta$  generation (Fig. 6). We also show that the decrease in APP endocytosis and insertion in Mint knockout neurons was fully rescued by viral expression of Mint1 (Fig. 7). We found that overexpression of individual Mints enhanced spontaneous synaptic transmission in excitatory neurons in addition to specifically altering APP trafficking (Figs. 8 and 9). Finally, we demonstrate a role for Mints in PS1 trafficking (Fig. 10). Mint knockout neurons display impaired PS1 endocytosis, which can be fully rescued by full-length Mint1. In contrast, the mutant Mint1 $\Delta$ PDZ1/2 fails to rescue, suggesting that the Mint1 interaction with PS1 is important in regulating PS1 trafficking. Furthermore, we show that enhanced synaptic activity facilitates the convergence of APP/PS1 colocalization, which requires Mints. Together, these findings demonstrate that Mint-dependent mechanisms, which are known to control synaptic transmission, also control activity-dependent APP and PS1 trafficking.

Endocytic trafficking of APP is required for synaptic activity-dependent  $A\beta$  production and secretion (22). However, the molecular and cellular mechanism(s) by which activity modulates APP endocytosis and  $A\beta$  production are less defined. Previous studies have demonstrated that Arc protein, best known for its role in glutamate receptor trafficking and synaptic plasticity, is essential for activity-dependent  $A\beta$  production (23). It

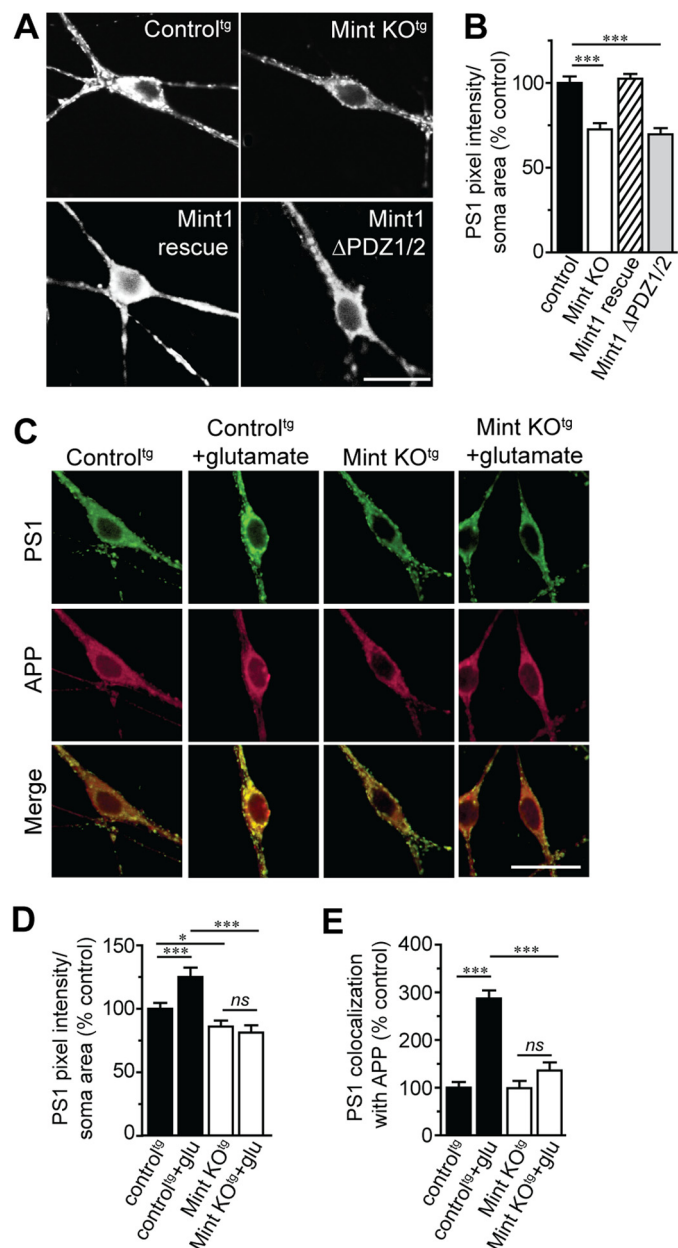


**FIGURE 10. Mints are required for PS1 internalization and activity-dependent colocalization with APP.** A and B, live cell endocytosis assay of MTF19 control, Mint KO, Mint1 rescue, and Mint1 truncated PDZ1/2 (*Mint1 $\Delta$ PDZ1/2*) mutant neurons labeled with an extracellular PS1 antibody. Internalized PS1 immunostaining was quantified as a measure of pixel intensity within defined somas and expressed as percent control ( $n = 2/199$  represents the number of independent experiments/total number of neurons assessed). C, representative images of live cell PS1 endocytosis assay and immunostaining with APP following glutamate application. *glu*, glutamate. D, PS1 immunostaining was quantified as a measure of pixel intensity within defined somas and expressed as percent control ( $n = 2/87$ ). E, colocalization of internalized PS1 with APP quantified within defined somas using Mander's coefficient ( $n = 2/168$ ). Scale bars = 20  $\mu\text{m}$  (somas). \*,  $p < 0.05$ ; \*\*\*,  $p < 0.001$ ; ns, not significant.

has been shown that Arc does not directly affect APP endocytosis from the plasma membrane. Instead, Arc binds to PS1 and associates with recycling endosomes, suggesting that Arc assists in sorting  $\gamma$ -secretase to early and recycling endosomes to process APP. Here we show that Mints are essential for activity-dependent APP endocytic trafficking. We analyzed primary neurons from three independent mouse lines to characterize



## Activity-dependent APP Trafficking by Mints

the effect of Mints on activity-dependent APP trafficking: conditional deletion of Mints from MTF, MTF<sup>tg</sup> carrying the double transgene *APP<sup>swe</sup>/PS1 $\Delta$ E9*, and wild-type overexpression experiments. Because it has been shown that wild-type APP sorting pathways differ from that of mutant APP<sup>swe</sup> (24, 25), it was important to compare endogenous APP and mutant APP<sup>swe</sup> trafficking pathways in response to changes in neuronal activity. We uncovered similar phenotypes in APP trafficking with endogenous APP and mutant APP<sup>swe</sup>. Neuronal stimulation increased APP endocytosis, whereas inhibition of neuronal activity decreased APP endocytosis, demonstrating a direct relationship between neuronal activity and APP endocytosis. The intracellular APP immunoreactive puncta were shown in both the somas and processes of primary neurons, suggesting that APP is sorted to both axonal and somatodendritic compartments. Previous studies have shown that APP is sorted equally to both presynaptic and postsynaptic compartments in primary neurons (26, 27). These changes were independent of alterations at the cell surface, suggesting that membrane insertion of APP could be regulated by neuronal activity. In fact, we found an increase in newly inserted APP staining on the surface, representing a rapid constitutive insertion of APP into the plasma membrane in response to glutamate activation, whereas TTX decreased APP insertion. The finding that activity-dependent APP endocytosis was blocked in Mint knockout neurons and was fully rescued with wild-type Mint1 strongly suggests that Mints are essential for activity-induced APP trafficking.

Recent studies have shown activity-induced convergence of APP and BACE1 via an endocytosis-dependent pathway to facilitate APP processing and A $\beta$  generation (28). Here, we show that APP and PS1 converge in an activity-dependent manner that requires Mints. In the past, adaptor proteins have been regarded to play a passive role in tethering proteins for cellular signaling and function. However, it is now clearly recognized that they play a dynamic role in finely tuning cellular information and responses (29, 30). Mint1 and Mint2 play more sophisticated roles in achieving functional regulation through autoinhibitory mechanisms (31, 32). We have shown previously that Mint1 undergoes a conformational switch between a “closed” state that does not bind APP and an “open” state involved in APP binding and that this switch plays a central role in regulating A $\beta$  production (31). In addition, previous NMR studies observed intramolecular contacts between the Mint1 C-terminal tail and the PDZ1 domain, which blocks its ability to bind exogenous targets such as PS1 (33). The discovery that Mint1 binding to APP and PS1 is regulated intramolecularly by autoinhibition generates valuable clues as to how a multidomain adaptor protein controls diverse neuronal signaling processes. However, further work is needed to determine what regulates Mint1 autoinhibition. It is plausible that activity-driven mechanisms induce conformational changes in the Mint1 protein and promote APP and PS1 binding and trafficking convergence in endocytic compartments, enhancing A $\beta$  generation.

APP trafficking in response to direct stimulation of glutamate or TTX may differ from physiological changes. For example, we have shown that phosphorylation of Mints by Src kinase stimulates APP trafficking (13). Phosphorylation of Mint2

accelerates APP endocytosis and sorts APP predominantly to LC3-positive autophagosomes, whereas phospho-resistant Mint2 sorts APP to the recycling pathway, back to the plasma membrane to facilitate APP processing and enhance A $\beta$  secretion. These studies demonstrate Src-mediated phosphorylation of Mint2 in regulating the APP endocytic sorting pathway, providing a mechanism for regulating A $\beta$  generation. Recently, it has been reported that polarized trafficking of *Drosophila* APP-like protein to axons is dependent on *Drosophila* Mint proteins through endocytosis in dendrites of the *Drosophila* mushroom body (34). This raises the question of whether Mints directly regulate endocytosis or act cooperatively with endocytosis to control specific membrane proteins that interact with Mints, such as APP. Our results indicate that Mints specifically affect the endocytosis of cell surface APP because activity-dependent, AMPA-type GluR1 internalization was not affected in Mint knockout neurons. Although previous studies have shown that elevated A $\beta$  attenuates excitatory synaptic transmission by decreasing the number of surface glutamate AMPA and NMDA receptors via endocytosis (1, 35, 36), we did not detect any changes in AMPA-type GluR1 receptor trafficking in primary neurons carrying mutant APP<sup>swe</sup> compared with wild-type neurons (data not shown). This is partly due to the fact that neuronal cultures are derived from postnatal day 1 pups, and mice at this age do not yet contain toxic amounts of A $\beta$  species, such as soluble oligomers or insoluble amyloid plaques, that interfere with excitatory synaptic transmission.

Neurons overexpressing individual Mint proteins showed a significant increase in both miniature event frequency and amplitude in excitatory synapses compared with control neurons, suggesting that overexpression of Mints alters the number of functional synapses either at presynaptic and/or postsynaptic sites. Interestingly, the levels of Mint1 are increased in the hippocampi of rats with epilepsy (37), and studies have shown that seizure activity is increased in AD and is associated with early amyloid deposition (38). Thus, it is conceivable that the increased expression of Mints found in AD patients (16, 17) can lead to changes in synaptic activity in addition to an increase in APP trafficking and A $\beta$  generation. Therefore, a detailed delineation of APP trafficking is an invaluable tool for future targeted therapeutics.

---

*Acknowledgments*—We thank Drs. T. C. Südhof and H. Man for plasmids and antibodies; Dr. U. Beffert, Dr. Z. Pang, and M. Toomey for comments and suggestions; and Dr. T. Blute and J. P. Gilbert for technical advice and assistance.

---

## REFERENCES

1. Kamenetz, F., Tomita, T., Hsieh, H., Seabrook, G., Borchelt, D., Iwatsubo, T., Sisodia, S., and Malinow, R. (2003) APP processing and synaptic function. *Neuron* **37**, 925–937
2. Cirrito, J. R., Deane, R., Fagan, A. M., Spinner, M. L., Parsadanian, M., Finn, M. B., Jiang, H., Prior, J. L., Sagare, A., Bales, K. R., Paul, S. M., Zlokovic, B. V., Piwnicka-Worms, D., and Holtzman, D. M. (2005) P-glycoprotein deficiency at the blood-brain barrier increases amyloid- $\beta$  deposition in an Alzheimer disease mouse model. *J. Clin. Invest.* **115**, 3285–3290
3. Cirrito, J. R., Yamada, K. A., Finn, M. B., Sloviter, R. S., Bales, K. R., May, P. C., Schoepp, D. D., Paul, S. M., Mennerick, S., and Holtzman, D. M. (2005) Synaptic activity regulates interstitial fluid amyloid- $\beta$  levels *in vivo*.

- Neuron* **48**, 913–922
4. Groemer, T. W., Thiel, C. S., Holt, M., Riedel, D., Hua, Y., Hüve, J., Wilhelm, B. G., and Klingauf, J. (2011) Amyloid precursor protein is trafficked and secreted via synaptic vesicles. *PLoS ONE* **6**, e18754
  5. Haass, C., Hung, A. Y., Selkoe, D. J., and Teplow, D. B. (1994) Mutations associated with a locus for familial Alzheimer's disease result in alternative processing of amyloid  $\beta$ -protein precursor. *J. Biol. Chem.* **269**, 17741–17748
  6. Koo, E. H., and Squazzo, S. L. (1994) Evidence that production and release of amyloid  $\beta$ -protein involves the endocytic pathway. *J. Biol. Chem.* **269**, 17386–17389
  7. Ring, S., Weyer, S. W., Kilian, S. B., Waldron, E., Pietrzik, C. U., Filippov, M. A., Herms, J., Buchholz, C., Eckman, C. B., Korte, M., Wolfer, D. P., and Müller, U. C. (2007) The secreted  $\beta$ -amyloid precursor protein ectodomain APPs $\alpha$  is sufficient to rescue the anatomical, behavioral, and electrophysiological abnormalities of APP-deficient mice. *J. Neurosci.* **27**, 7817–7826
  8. Okamoto, M., and Südhof, T. C. (1997) Mints, Munc18-interacting proteins in synaptic vesicle exocytosis. *J. Biol. Chem.* **272**, 31459–31464
  9. Borg, J. P., Ooi, J., Levy, E., and Margolis, B. (1996) The phosphotyrosine interaction domains of X11 and FE65 bind to distinct sites on the YENPTY motif of amyloid precursor protein. *Mol. Cell. Biol.* **16**, 6229–6241
  10. Lau, K. F., McLoughlin, D. M., Standen, C. L., Irving, N. G., and Miller, C. C. (2000) Fe65 and X11 $\beta$  co-localize with and compete for binding to the amyloid precursor protein. *Neuroreport* **11**, 3607–3610
  11. Biederer, T., Cao, X., Südhof, T. C., and Liu, X. (2002) Regulation of APP-dependent transcription complexes by Mint/X11s: differential functions of Mint isoforms. *J. Neurosci.* **22**, 7340–7351
  12. Ho, A., Liu, X., and Südhof, T. C. (2008) Deletion of Mint proteins decreases amyloid production in transgenic mouse models of Alzheimer's disease. *J. Neurosci.* **28**, 14392–14400
  13. Chaufy, J., Sullivan, S. E., and Ho, A. (2012) Intracellular amyloid precursor protein sorting and amyloid- $\beta$  secretion are regulated by Src-mediated phosphorylation of Mint2. *J. Neurosci.* **32**, 9613–9625
  14. Ho, A., Morishita, W., Atasoy, D., Liu, X., Tabuchi, K., Hammer, R. E., Malenka, R. C., and Südhof, T. C. (2006) Genetic analysis of Mint/X11 proteins: essential presynaptic functions of a neuronal adaptor protein family. *J. Neurosci.* **26**, 13089–13101
  15. Ho, A., Morishita, W., Hammer, R. E., Malenka, R. C., and Südhof, T. C. (2003) A role for Mints in transmitter release: Mint 1 knockout mice exhibit impaired GABAergic synaptic transmission. *Proc. Natl. Acad. Sci. U.S.A.* **100**, 1409–1414
  16. Jacobs, E. H., Williams, R. J., and Francis, P. T. (2006) Cyclin-dependent kinase 5, Munc18a and Munc18-interacting protein 1/X11 $\alpha$  protein up-regulation in Alzheimer's disease. *Neuroscience* **138**, 511–522
  17. McLoughlin, D. M., Irving, N. G., Brownlee, J., Brion, J. P., Leroy, K., and Miller, C. C. (1999) Mint2/X11-like colocalizes with the Alzheimer's disease amyloid precursor protein and is associated with neuritic plaques in Alzheimer's disease. *Eur. J. Neurosci.* **11**, 1988–1994
  18. Rhinn, H., Fujita, R., Qiang, L., Cheng, R., Lee, J. H., and Abeliovich, A. (2013) Integrative genomics identifies APOE  $\epsilon$ 4 effectors in Alzheimer's disease. *Nature* **500**, 45–50
  19. Beffert, U., Dillon, G. M., Sullivan, J. M., Stuart, C. E., Gilbert, J. P., Kambouris, J. A., and Ho, A. (2012) Microtubule plus-end tracking protein CLASP2 regulates neuronal polarity and synaptic function. *J. Neurosci.* **32**, 13906–13916
  20. Perez, R. G., Squazzo, S. L., and Koo, E. H. (1996) Enhanced release of amyloid  $\beta$ -protein from codon 670/671 "Swedish" mutant  $\beta$ -amyloid precursor protein occurs in both secretory and endocytic pathways. *J. Biol. Chem.* **271**, 9100–9107
  21. Thinakaran, G., Teplow, D. B., Siman, R., Greenberg, B., and Sisodia, S. S. (1996) Metabolism of the "Swedish" amyloid precursor protein variant in neuro2a (N2a) cells. Evidence that cleavage at the " $\beta$ -secretase" site occurs in the Golgi apparatus. *J. Biol. Chem.* **271**, 9390–9397
  22. Cirrito, J. R., Kang, J. E., Lee, J., Stewart, F. R., Verges, D. K., Silverio, L. M., Bu, G., Mennerick, S., and Holtzman, D. M. (2008) Endocytosis is required for synaptic activity-dependent release of amyloid- $\beta$  *in vivo*. *Neuron* **58**, 42–51
  23. Wu, J., Petralia, R. S., Kurushima, H., Patel, H., Jung, M. Y., Volk, L., Chowdhury, S., Shepherd, J. D., Dehoff, M., Li, Y., Kuhl, D., Haganir, R. L., Price, D. L., Scannevin, R., Troncoso, J. C., Wong, P. C., and Worley, P. F. (2011) Arc/Arg3.1 regulates an endosomal pathway essential for activity-dependent  $\beta$ -amyloid generation. *Cell* **147**, 615–628
  24. Haass, C., Koo, E. H., Capell, A., Teplow, D. B., and Selkoe, D. J. (1995) Polarized sorting of  $\beta$ -amyloid precursor protein and its proteolytic products in MDCK cells is regulated by two independent signals. *J. Cell Biol.* **128**, 537–547
  25. Huse, J. T., Pijak, D. S., Leslie, G. J., Lee, V. M., and Doms, R. W. (2000) Maturation and endosomal targeting of  $\beta$ -site amyloid precursor protein-cleaving enzyme. The Alzheimer's disease  $\beta$ -secretase. *J. Biol. Chem.* **275**, 33729–33737
  26. Back, S., Haas, P., Tschäpe, J. A., Gruebl, T., Kirsch, J., Müller, U., Beyreuther, K., and Kins, S. (2007)  $\beta$ -Amyloid precursor protein can be transported independent of any sorting signal to the axonal and dendritic compartment. *J. Neurosci. Res.* **85**, 2580–2590
  27. Hoey, S. E., Williams, R. J., and Perkinson, M. S. (2009) Synaptic NMDA receptor activation stimulates  $\alpha$ -secretase amyloid precursor protein processing and inhibits amyloid- $\beta$  production. *J. Neurosci.* **29**, 4442–4460
  28. Das, U., Scott, D. A., Ganguly, A., Koo, E. H., Tang, Y., and Roy, S. (2013) Activity-induced convergence of APP and BACE-1 in acidic microdomains via an endocytosis-dependent pathway. *Neuron* **79**, 447–460
  29. Good, R. L., Liang, L. P., Patel, M., and Radcliffe, R. A. (2011) Mouse strain- and age-dependent effects of binge methamphetamine on dopaminergic signaling. *Neurotoxicology* **32**, 751–759
  30. Pawson, T. (2007) Dynamic control of signaling by modular adaptor proteins. *Curr. Opin. Cell Biol.* **19**, 112–116
  31. Matos, M. F., Xu, Y., Dulubova, I., Otwinowski, Z., Richardson, J. M., Tomchick, D. R., Rizo, J., and Ho, A. (2012) Autoinhibition of Mint1 adaptor protein regulates amyloid precursor protein binding and processing. *Proc. Natl. Acad. Sci. U.S.A.* **109**, 3802–3807
  32. Xie, H., Hou, S., Jiang, J., Sekutowicz, M., Kelly, J., and Bacskaï, B. J. (2013) Rapid cell death is preceded by amyloid plaque-mediated oxidative stress. *Proc. Natl. Acad. Sci. U.S.A.* **110**, 7904–7909
  33. Long, J. F., Feng, W., Wang, R., Chan, L. N., Ip, F. C., Xia, J., Ip, N. Y., and Zhang, M. (2005) Autoinhibition of X11/Mint scaffold proteins revealed by the closed conformation of the PDZ tandem. *Nat. Struct. Mol. Biol.* **12**, 722–728
  34. Gross, G. G., Lone, G. M., Leung, L. K., Hartenstein, V., and Guo, M. (2013) X11/Mint genes control polarized localization of axonal membrane proteins *in vivo*. *J. Neurosci.* **33**, 8575–8586
  35. Hsieh, H., Boehm, J., Sato, C., Iwatsubo, T., Tomita, T., Sisodia, S., and Malinow, R. (2006) AMPAR removal underlies  $\beta$ A $\beta$ -induced synaptic depression and dendritic spine loss. *Neuron* **52**, 831–843
  36. Shankar, G. M., Bloodgood, B. L., Townsend, M., Walsh, D. M., Selkoe, D. J., and Sabatini, B. L. (2007) Natural oligomers of the Alzheimer amyloid- $\beta$  protein induce reversible synapse loss by modulating an NMDA-type glutamate receptor-dependent signaling pathway. *J. Neurosci.* **27**, 2866–2875
  37. Scorza, C. A., Garrido Ydel, C., Arida, R. M., Amado, D., Cavalheiro, E. A., and Naffah-Mazzacoratti Mda, G. (2003) Levels of the synaptic protein X11  $\alpha$ /mint1 are increased in hippocampus of rats with epilepsy. *Epilepsy Res.* **57**, 49–57
  38. Amatniek, J. C., Hauser, W. A., DelCastillo-Castaneda, C., Jacobs, D. M., Marder, K., Bell, K., Albert, M., Brandt, J., and Stern, Y. (2006) Incidence and predictors of seizures in patients with Alzheimer's disease. *Epilepsia* **47**, 867–872